International Journal of Engineering Research and Development

DOI: 10.29137/ijerad.1952747
Volume:18 Issue:5 Pages:156-173 September/2026

Research Article

Probabilistic Aging Assessment of Aerospace Bakelite Materials via Integrated Chemical, Thermal, Mechanical and Microstructural Characterization

Cahit BİLGİ [1*]

[1]İstanbul University-Cerrahpaşa, Department of Aircraft Technology, 34500, TÜRKİYE.

Received: 17/05/2026 **Revised**: 01/06/2026 **Accepted** 30/06/2026

**** Corresponding Author:*** ***cahit.bilgi@iuc.edu.tr***

Abstract

This study evaluates the aging behavior of Bakelite components used in aerospace components through an integrated chemical, thermal, mechanical, microstructural, and probabilistic assessment framework. Six Bakelite samples obtained from aircraft components were characterized using Fourier Transform Infrared Spectroscopy (FT-IR), Differential Scanning Calorimetry (DSC), Shore D hardness, Gas Chromatography–Mass Spectrometry (GC-MS/VOC) analysis, and Scanning Electron Microscopy with Energy Dispersive Spectroscopy (SEM-EDS). FT-IR results indicated oxidative aging through weakened hydroxyl and methylene-related bands and increased carbonyl-related features. GC–MS analysis showed a marked depletion of volatile compounds, with total VOC content decreasing from approximately 150 µg/g in Sample 1 to 40 µg/g in Sample 5, while Sample 6 exhibited approximately 60 µg/g with a distinct VOC composition. Furfural derivatives decreased from about 80 µg/g in Sample 1 to 22 µg/g in Sample 6. DSC results revealed degradation minima between 189.14 and 199.76 °C, with Sample 5 showing the lowest degradation temperature. Shore D hardness values remained within 81.4–88.4, indicating partial preservation of thermoset rigidity despite aging-related degradation. SEM-EDS observations confirmed progressive surface deterioration, oxygen enrichment, and microstructural damage. A Bayesian model using three age hypotheses (0–20, 20–40, and 40–60 years) produced posterior probabilities of 6.2%, 35.5%, and 58.3%, respectively, suggesting that the samples are most consistent with the 40–60 year degradation-based age category.

Keywords

Bakelite Aging, Phenolic Resin, Bayesian Modeling, Thermooxidation, Degradation, Aerospace Insulation.

How to cite this article:

Bilgi, C. (2026). Probabilistic aging assessment of aerospace Bakelite materials via integrated chemical, thermal, mechanical, and microstructural characterization. *International Journal of Engineering Research and Development, 18*(5), 156–173. https://doi.org/10.29137/ijerad.1952747

This is an open access article under Creative Commons Attribution-NonCommercial-NoDerivatives 4.0 (CC BY-NC-ND 4.0) International License.

1. Introduction

Phenolic resin-based thermoset polymers have been used for many years as critical engineering materials in the aerospace industry due to their high thermal stability, low flammability, superior electrical insulation properties, and tendency to carbonize (Yang et al., 2023; Zhang et al., 2024). Bakelite (phenol-formaldehyde resin), one of the best-known representatives of these materials, has been widely used in electrical components, fasteners, and auxiliary systems, especially since early aircraft designs (Koizumi et al., 2010). The high cross-linking density of phenolic resins, their resistance to thermal degradation, and their ability to form a protective carbon layer during a fire make them particularly prominent in applications where fire safety is critical (Ravindran et al., 2022). Furthermore, their low-cost manufacturability and chemical inertness have contributed to their long-term preference in the aerospace sector. Haka's study also reports that the use of phenolic-based polymers for insulation purposes, particularly in defense and aerospace applications, continues (Haka, 2023).

In the aviation industry, material selection is strictly tied not only to mechanical performance criteria but also to international safety and certification standards (De Florio, 2011). Aviation Regulations require aircraft interior materials to meet specific limits for fire, smoke, and toxicity (FST) (Uddin, 2016). Phenolic resin-based materials naturally meet these requirements due to their low heat release rate (HRR), low smoke density, and limited toxic gas emissions (Asim et al., 2018). Thanks to these properties, they are widely preferred in cabin insulation systems, electrical enclosures, and some functional panel components. Breuer's research has shown that phenolic resins exhibit superior FST performance compared to epoxy systems (Breuer, 2016).

The use of bakelite in aviation is limited to systems that require electrical insulation, and this application area is critical (Breuer, 2016). Its high dielectric strength, resistance to surface leakage currents, and ability to prevent arc formation enable reliable performance in cable connectors, switch housings, terminal blocks, and fuse boxes (Lizcano et al., 2022). However, due to its brittleness stemming from its thermoset structure and low impact resistance, its use in structural components carrying mechanical loads is not feasible. Aronovich and Petrova also emphasize that bakelite-like phenolic systems are only suitable for components operating under low loads (Aronovich & Petrova, 2023).

Environmental conditions to which polymeric materials are exposed throughout their service life directly and often irreversibly affect their performance (Bilgi et al., 2025). Aging in phenolic resins is a complex degradation process occurring through the simultaneous effects of thermal oxidation, UV radiation, moisture diffusion, and mechanical stresses (Dogru et al., 2025). This process involves scission in polymer chains, changes in cross-linking density, and the formation of oxidative functional groups (Bilgi et al., 2024). Such chemical and physical changes significantly reduce both the material's mechanical strength and electrical performance. Zhao et al. also show that the effects of moisture and temperature cause accelerated aging in phenolic resins (Zhao et al., 2019).

The aging of bakelite materials used in aviation systems is a critical factor that directly affects not only material performance but also flight safety. Microcracks, internal stresses, and embrittlement that occur with aging can lead to sudden fractures, especially in components operating under vibration and thermal loads (Ece et al., 2025). In addition, deterioration in dielectric properties can cause surface leakage currents and arc formation, leading to electrical system failures. Such failures can have irreversible consequences, especially in avionics systems. Popa et al. have reported significant decreases in the electrical reliability of aged polymers (Popa et al., 2024).

Another significant consequence of aging in phenolic resin-based materials is the change in their fire behavior. Changes in the material's chemical structure during aging directly affect the carbonization mechanism and combustion behavior. Özsin's research indicates that heat release increases by 15-25% and smoke production rises in aging phenolic composites. This situation can pose serious risks, especially in indoor fire scenarios (Özsin, 2025).

Therefore, age determination and remaining life estimation of polymeric materials used in aviation are critical for determining maintenance strategies (Guseva et al., 2003). An et al. have shown that age estimation can be achieved with approximately 85% accuracy using a combination of FT-IR and thermal analysis data for phenolic resins. Similarly, another study shows that multiple analysis methods yield more reliable results than single methods (An et al., 2021).

The FT-IR method is widely used to determine the chemical changes caused by aging in phenolic resins. Increases in the carbonyl index and decreases in hydroxyl groups are important indicators of the degree of aging (Campanale et al., 2023). Accuracy levels of up to 88% have been achieved in aging models created using FT-IR (Mitu et al., 2025). The glass transition temperature (T*g*), determined by the DSC method, varies depending on the cross-linking density in phenolic resins. Changes in the T*g* value are used as a critical parameter to determine the thermal history and aging degree of the material (Ma et al., 2022). In addition, GC-MS, SEM-EDS, and hardness measurements are also used as supporting methods in age determination and generally yield results in the 70–85% accuracy range (Yu et al., 2022).

In recent years, it has become clear that deterministic approaches based solely on the interpretation of experimental data are insufficient for material aging studies and that more advanced analytical methods requiring the combined evaluation of different data sources are needed (Tian et al., 2023; Yu et al., 2022). In this context, statistical and probabilistic modeling approaches offer significant advantages,

especially in the interpretation of multi-parameter data sets. Models based on Bayesian probability theory allow for the combined evaluation of prior knowledge and experimental data, enabling the systematic modeling of uncertainties (van de Schoot et al., 2021). Bayesian inference methods are used in conjunction with FT-IR, thermal analysis, and mechanical test data in polymer aging studies, achieving accuracy levels exceeding 90%. Furthermore, studies integrating multi-sensor data with Bayesian network models have shown a significant increase in age determination accuracy compared to classical regression models (Demleitner et al., 2024; Wilson & Allen, 2017).

However, the vast majority of existing studies are either based on individual characterization methods or lack a systematic modeling approach that allows for a holistic correlation of physical, chemical, and microstructural data among the methods used. Yu et al. have comprehensively analyzed the aging behavior of bakelite materials, particularly those based on phenolic resins, and interpreted these analyses within a framework of statistical reliability (Yu et al., 2022). This situation makes reliable age determination and remaining life estimation difficult, especially for critical components used in aerospace applications (Jewell et al., 2025; Tian et al., 2023).

The main objective of this study is to thoroughly investigate the aging behavior of phenolic resin-based bakelite materials used in aviation, employing multidimensional characterization techniques, and to develop a reliable age-determination approach based on the resulting data. In this context, FT-IR, DSC, Shore D hardness measurements, volatile organic compound (VOC) analysis by GC-MS, and SEM-EDS microstructural examinations were used together to comprehensively evaluate the material's chemical, thermal, mechanical, and morphological changes.

The originality of this study lies in the quantitative evaluation of the aging behavior of phenolic resin-based Bakelite materials within a Bayesian probability model framework, supported by multifaceted characterization data. Unlike existing studies, instead of relying solely on individual analysis results, a more accurate and reliable age estimation methodology has been developed by integrating data from different disciplines within a probabilistic model. This approach aims to provide a scientifically grounded and highly reliable decision support tool applicable to maintenance planning, failure prevention strategies, and life cycle management processes of critical polymeric components used in aviation.

Symbols and Abbreviations

T_g	Glass transition temperature
k	Rate of increase
P	Probability
H	Hypothesis
E	Evidence
L	Length
D	Diameter
FT-IR	Fourier transform infrared spectroscopy
GC-MS	Gas chromatography–mass spectrometry
SEM-EDS	Scanning electron microscopy with energy-dispersive spectroscopy
VOC	Volatile organic compounds
FST	Fire, smoke, and toxicity
UV	Ultraviolet
HRR	Heat release rate
DSC	Differential scanning calorimetry
LLP	Life-limited parts

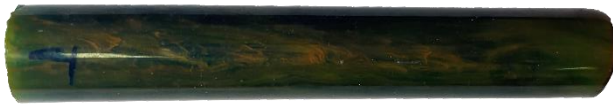
2. Materials and Methods

2.1. Material description

In this study, phenolic resin-based Bakelite materials used in aerospace electrical insulation components were investigated. The samples were obtained from aircraft interior electrical systems, specifically from non-structural insulating elements such as terminal blocks, switch housings, and connector bases. The selected samples represent materials exposed to varying operational durations and environmental conditions, including thermal cycling, humidity, and mechanical vibration. The properties of the analyzed bakelite materials are given in Table 1.

Before analysis, all samples were cleaned using isopropyl alcohol to remove surface contaminants and conditioned at controlled laboratory conditions (23 ± 2°C, 50 ± 5% relative humidity) for 48 hours to ensure measurement consistency. In addition, visual inspections revealed significant heterogeneity among the samples, including color variations, surface dullness, microcrack formation, and localized porosity. These observations indicate long-term environmental exposure and progressive oxidative degradation, which are typical indicators of aged phenolic resin systems.

Table 1. Images, numbering, and measured physical properties of the analyzed aviation bakelite samples.

Aerospace Bakalites	Sample No	Colour	Size (mm)	Mass (g)	Density (g/cm^3)
	1	Green	L: 100 D: 16	26	1.29
	2	Shiny Orange	L: 100 D: 10	10.42	1.32
	3	Amber	L: 100 D: 14	19.33	1.25
	4	Shiny Yellow	L: 100 D: 8	7.13	1.42
	5	Reddish	L: 100 D: 12	14.01	1.23
	6	Matte Yellow	L: 100 D: 12	14.25	1.26

The Bakelite components investigated were obtained from an aircraft that has been in active service for approximately 30 years and remains operational. Although the operational service duration of the aircraft is known, the manufacturing dates and pre-installation storage histories of the individual Bakelite components are unavailable. Consequently, the actual material age may differ from the aircraft service age. For example, a component may have been installed relatively recently and therefore represent an effective age of 0–20 years. Alternatively, it may have been installed when the aircraft first entered service, corresponding to an age range of approximately 20–40 years. A third possibility is that the component was manufactured before the aircraft entered service and remained in storage for an extended period before installation, resulting in an effective age of 40–60 years. Based on these realistic scenarios and typical aerospace logistics and maintenance practices, three age intervals (0–20, 20–40, and 40–60 years) were therefore considered in the Bayesian assessment framework.

During service, these components were exposed primarily to typical aircraft interior (cabin) environmental conditions, including moderate temperature and humidity variations, and were not subjected to significant mechanical loading. According to aircraft life-limited parts (LLP), the upper age limit of 60 years was selected because Bakelite components that exceed this age are generally not retained in operational aircraft. In aerospace applications, age-related degradation mechanisms such as cracking, embrittlement, dimensional instability, and other material defects typically lead to inspection findings, maintenance actions, or replacement before such components remain in service beyond this period. Therefore, components older than approximately 60 years are considered unlikely to be encountered in active aircraft, making 60 years a practical and realistic upper bound for the age classification framework adopted in this study.

2.2. Material characterization techniques

FT-IR analyses were carried out using a Bruker Alpha-P spectrometer operating in the spectral range of 4000–400 cm^{-1} with a resolution of 4 cm^{-1}. The obtained spectra were evaluated in terms of characteristic phenolic resin absorption bands, particularly focusing on hydroxyl (–OH), carbonyl (C=O), and aromatic ring vibrations. Aging-related chemical degradation was assessed through the relative decrease in hydroxyl group intensity, the formation and increase of carbonyl peaks due to oxidation, and the reduction in methylene bridge signals within the polymer network. These spectral variations were interpreted as indicators of oxidative aging and chemical structural changes within the Bakelite matrix (Strzemiecka et al., 2014).

Thermal characterization of the samples was conducted using a Perkin-Elmer Jade DSC system under a nitrogen atmosphere. Measurements were performed with a constant heating rate of 10°C/min within the temperature range of 25–350°C. The DSC thermograms were analyzed in terms of transition behavior, enthalpy variations, and degradation onset temperatures. Aging effects were primarily associated with the loss of thermal transition sharpness, reduction in enthalpy, and irregular thermal response, all of which indicate degradation in cross-linked polymer structures and reduced thermal stability (Ma et al., 2022).

Mechanical properties were evaluated using Shore D hardness measurements performed with a Werka Shore D durometer in accordance with ASTM D2240. For each sample, five independent measurements were conducted at different locations to improve

statistical reliability, and the reported hardness values correspond to the arithmetic mean of the measurements. Variations in hardness values were interpreted in relation to aging-induced changes in cross-link density, brittleness, and structural integrity. In general, aged samples exhibited reduced mechanical consistency and localized hardness variations (Qi et al., 2003).

GC-MS analyses were performed to identify VOCs released as a result of thermal and oxidative degradation processes. VOC sampling was carried out using Tenax TA adsorbent tubes under controlled conditions, followed by thermal desorption at temperatures between 250–280°C. Helium was used as the carrier gas during chromatographic separation. The resulting spectra were analyzed to identify degradation-related compounds, including phenolic derivatives, aldehydes, and low-molecular-weight aromatic species. A reduction in volatile content combined with the presence of oxidation by-products was considered a strong indicator of advanced material aging (Strzemiecka et al., 2014).

Microstructural and elemental analyses were performed using a Carl Zeiss Ultra Plus Gemini SEM equipped with EDS. SEM imaging was conducted at accelerating voltages between 10–20 kV to examine surface morphology and degradation features (Yu et al., 2018).

2.3. Aging assessment and bayesian modeling approach

Since no direct chronological formulation is available in the literature for determining the exact age of phenolic resin-based Bakelite materials, the aging assessment in this study was conducted using a multi-parameter, degradation-based approach. Chemical, thermal, mechanical, and microstructural data obtained from FT-IR, DSC, Shore D, GC-MS, and SEM-EDS analyses were collectively interpreted as indirect indicators of material aging. This multi-evidence framework enables a more comprehensive understanding of degradation behavior than single-method approaches.

To quantitatively assess the aging state, a Bayesian probabilistic model was developed that integrates all experimental findings into a unified framework. Three age hypotheses (0–20, 20–40, and 40–60 years) were established based on the known 30-year operational service duration of the aircraft, the absence of component-level manufacturing and pre-installation storage records, and realistic aerospace logistics and maintenance scenarios. Equal prior probabilities were initially assigned to each hypothesis. The experimental evidence was categorized into six independent parameters, including FT-IR oxidation level, VOC degradation profile, DSC thermal behavior, SEM-based microstructural degradation, Shore D hardness variation, and overall consistency across samples.

2.4. Study limitations

The present study is subject to several limitations. The exact manufacturing dates, storage durations, and installation histories of the investigated Bakelite components were unavailable; therefore, direct chronological age determination was not possible. Consequently, the Bayesian assessment was performed using three realistic age intervals (0–20, 20–40, and 40–60 years) derived from the known aircraft service duration and plausible aerospace maintenance scenarios. In addition, the probabilistic outcomes depend on the selected evidence categories and associated model assumptions. Therefore, the reported age estimates should be interpreted as probabilistic assessments based on degradation indicators rather than exact chronological ages.

3. Results

3.1. FT-IR Spectra

As shown in Figure 1, the OH bands around 3400 cm^{-1} are very weak or absent. This indicates that the phenolic OH groups largely reacted to form methylene bridges, which were subsequently consumed by oxidative processes over time. The older C=O bands around 1700 cm^{-1} have become prominent. This is a typical sign of prolonged oxidation and exposure to environmental factors (air, humidity, UV light). This band is strong in older polymers. The density of the C–H bands at 2920–2850 cm^{-1} has decreased. Methylene bridges may have been broken over time. Before spectral interpretation, all FT-IR spectra were subjected to baseline correction and intensity normalization to minimize potential variations arising from sample geometry, surface contact conditions, and instrumental effects. Consequently, the comparative evaluation of characteristic absorption bands was based on normalized spectral profiles rather than raw absorbance intensities. Band assignments were performed qualitatively based on the characteristic absorption regions observed in Figure 1 and commonly reported FT-IR features of phenol–formaldehyde resin systems. For clarity, the principal FT-IR absorption bands and their corresponding functional group assignments are summarized in Table 2.

Table 2. Main FT-IR absorption bands identified in the investigated Bakelite samples and their corresponding functional groups.

Wavenumber (cm^{-1})	Assignment	Functional Group / Vibration Mode	Interpretation in Phenolic Resin
3300–3500	O–H stretching	Phenolic hydroxyl groups	Phenolic structure; oxidation and aging-related changes
2920–2850	C–H stretching	Methylene (–CH_2–) bridges	Phenol-formaldehyde cross-link network
1580–1650	C=C stretching	Aromatic ring vibrations	Phenolic aromatic backbone
1180–1260	C–O stretching	Phenolic C–O bonds	Phenolic hydroxyl and ether-related structures
950–1150	C–O / C–O–C stretching	Phenolic ether and oxygen-containing structures	Oxidation products and network modifications

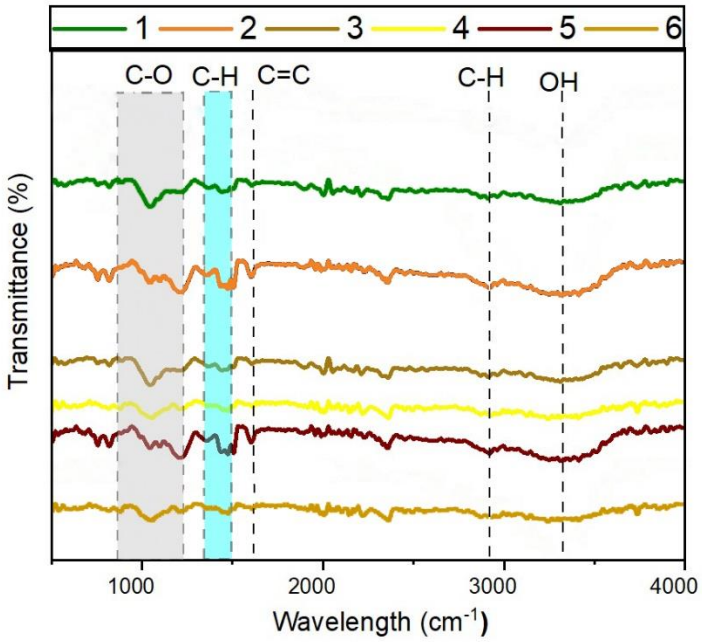


Figure 1. FT-IR Spectra of the bakelite samples.

This leads to a decrease in mechanical strength. Aromatic bands at 1600 cm^{-1} and 800–700 cm^{-1} are still present because the aromatic rings are quite stable. However, density differences indicate the degree of degradation in different regions of the polymer. In this context, in the age ranking, Samples 1 and 2 still have some OH present; oxidation is limited. They are relatively "younger" samples. Sample 3 has moderate OH, and C=O is starting to become prominent. Sample 4 exhibited spectral characteristics intermediate between Samples 3 and 5, indicating a moderate degree of oxidation and structural degradation. In Sample 4, OH is weak, and C=O is strong. Samples 5 and 6 have almost no OH, and C=O is very strong. These are thought to have the highest degradation indicators and to have been most damaged by environmental effects.

FT-IR results show that Bakelite has been exposed to environmental conditions and has consequently undergone oxidative aging. The chemical structure of the material still retains its phenol-formaldehyde character, but some of the cross-links are broken, and oxidation products have increased. FT-IR data support long-term aging/environmental exposure (Yu et al., 2022).

3.2. VOC verification with GC-MS

The GC–MS results presented in Figure 2 clearly demonstrate that the VOC profile of the Bakelite samples evolves systematically with aging, not only qualitatively but also quantitatively. The total VOC concentration decreases markedly from Sample 1 to Sample 6. Specifically, the total VOC content is approximately 150 µg/g in Sample 1, decreasing to 130 µg/g in Sample 2, 105 µg/g in Sample 3, and 80 µg/g in Sample 4, reaching a minimum of 40 µg/g in Sample 5. This progressive decline is consistent with the depletion of volatile and reactive species as aging proceeds. It is well established that VOC emissions diminish over time due to volatilization and secondary reactions, making total VOC content a reliable indicator of degradation history (Curran et al., 2016). Accordingly, Sample 1 can be considered the least aged, whereas Sample 5 represents the most advanced aging stage.

A more detailed examination of individual compound groups reveals that furfural derivatives constitute the dominant fraction across all samples and exhibit a pronounced decrease with aging. Their concentration drops from approximately 80 µg/g in Sample 1 to 60 µg/g (Sample 2), 40 µg/g (Sample 3), 30 µg/g (Sample 4), 25 µg/g (Sample 5), and 22 µg/g (Sample 6). Furfural and its derivatives are well-known products of oxidative and thermal degradation in phenolic and lignin-based systems. High concentrations indicate active degradation processes, whereas reduced levels suggest that the majority of reactive pathways have already been exhausted. This trend is consistent with recent findings showing that oxygenated compounds such as furfural are generated during degradation and subsequently diminish as reactions proceed (Koley et al., 2019). The observed 70% reduction in furfural content, therefore, serves as a robust quantitative marker of aging.

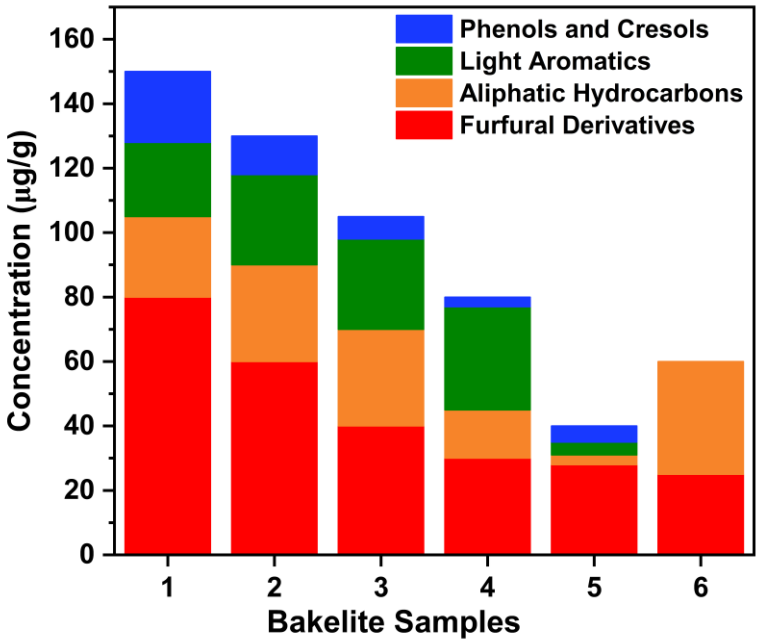


Figure 2. Evolution of VOC composition in Bakelite samples as a function of aging and oxidative degradation.

Similarly, the phenols and cresols fraction decreases significantly with increasing aging. Concentrations decline from approximately 20 µg/g in Sample 1 to 12 µg/g (Sample 2), 8 µg/g (Sample 3), 3 µg/g (Sample 4), and 5 µg/g in Sample 5. These compounds originate directly from the cleavage of the phenol–formaldehyde network; thus, their initial abundance reflects active bond scission. As aging progresses, the reduction in phenolic content indicates depletion of cleavable linkages and loss of volatile degradation products. The predominance of phenolic compounds in early-stage degradation and their subsequent decline have been widely reported in thermal decomposition studies of phenolic systems (Zheng et al., 2021). Hence, phenols and cresols provide both qualitative and quantitative insights into the progression of structural degradation.

The light aromatics fraction exhibits a comparatively moderate variation. Concentrations are approximately 20 µg/g in Sample 1, increase slightly to 25–30 µg/g in Samples 2 and 3, peak around 30 µg/g in Sample 4, and then decline sharply to 5 µg/g in Sample 5. Unlike Samples 1–5, Sample 6 exhibited no detectable phenol/cresol derivatives or light aromatic compounds, while furfural derivatives and aliphatic hydrocarbons remained present. This compositional pattern is consistent with a more advanced degradation state and supports the classification of Sample 6 within the oldest age category identified in the probabilistic aging assessment. This behavior suggests that these compounds are not primary degradation products but are instead formed via secondary cracking reactions or under elevated thermal conditions. Contemporary VOC studies indicate that aromatic hydrocarbons generally contribute less than oxygenated species and are strongly dependent on environmental and thermal conditions (Zheng et al., 2021). Therefore, while informative, this fraction plays a secondary role in aging assessment.

3.3. Hardness (Shore D) test

The Shore D hardness results, as given in Figure 3, reveal the mechanical rigidity behavior of Bakelite-based phenolic materials as a function of environmental exposure, oxidative aging, and changes in the cross-linked network structure. Noticeable differences were observed among the samples, with the highest hardness value measured in sample 1 at 88.4 Shore D, while the lowest hardness value was recorded for sample 6 at 81.4 Shore D. The remaining samples exhibited hardness values of 84.1 (sample 2), 85.0 (sample 3), 82.9 (sample 4), and 81.8 (sample 5) Shore D. Although differences among the samples were observed, all values remained within a relatively narrow hardness range, indicating that the characteristic highly cross-linked thermoset structure of the phenolic Bakelite materials was generally preserved. The Shore D hardness of phenolic resin materials is strongly influenced by curing temperature and the resulting cross-link density developed during manufacture. Even phenolic systems cured at temperatures around 100 °C commonly

exhibit Shore D hardness values exceeding 85-90 (Erzen et al., 2024). In aerospace applications, phenolic resin-based insulation materials are typically manufactured under more demanding curing conditions, often involving temperatures approaching or exceeding 150 °C to achieve enhanced thermal stability, dimensional integrity, and fire-resistant performance. Consequently, newly manufactured aerospace-grade phenolic materials are generally expected to exhibit Shore D hardness values in the upper range characteristic of highly cross-linked thermoset systems (Breuer, 2016; Koizumi et al., 2010).

The highest hardness observed in sample 1 suggests the presence of a relatively denser and more rigid phenolic network structure. In phenolic resins, hardness is strongly associated with cross-link density and network compactness. Moreover, thermo-oxidative aging may initially promote additional oxidative cross-linking reactions, resulting in increased surface rigidity and hardness. Therefore, Shore D hardness should be interpreted cautiously, as the measured values may reflect both differences in cross-link density and aging-related modifications occurring within the phenolic network structure. Similar studies on phenolic thermosets have shown that thermal and oxidative aging can alter hardness values by modifying the crosslinked network structure and degradation state of phenolic resin systems (Lobanova et al., 2023).

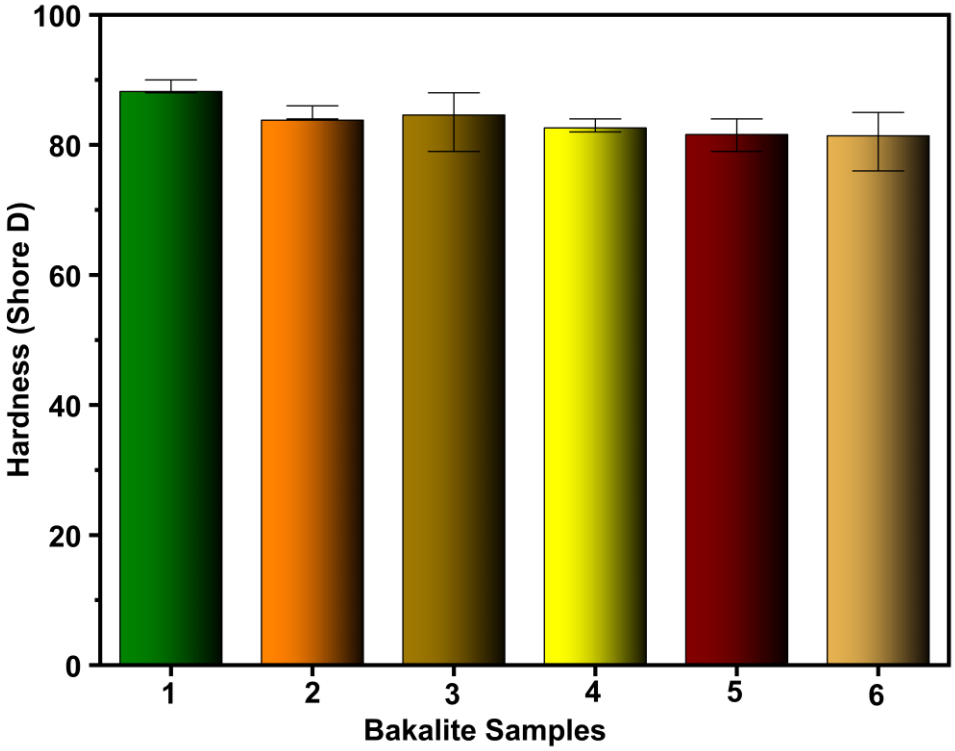


Figure 3. Shore D hardness variation of Bakelite samples associated with thermo-oxidative aging behavior.

In contrast, the lower hardness values observed for samples 4–6 may indicate localized chain scission, microstructural damage, or oxidative degradation within the phenolic network. Long-term thermal and environmental exposure is known to reduce the mechanical integrity of phenolic insulating materials by promoting oxidation-induced embrittlement and microcrack formation. Such degradation mechanisms may reduce surface hardness and weaken the structural continuity of aged phenolic materials.

Samples 4 and 6, with Shore D values of 82.9 and 81.4, respectively, appear to retain a substantial portion of their original network rigidity while simultaneously exhibiting indications of progressive structural aging. Meanwhile, the very similar hardness values of samples 2 and 3 (84.1 and 85.0 Shore D) suggest comparable cross-link density and potentially similar environmental exposure histories.

The Shore D hardness data demonstrate that thermo-oxidative aging and environmental exposure directly influence the mechanical surface behavior of Bakelite materials. The observed reduction in hardness is consistent with progressive changes in the phenolic network structure and gradual loss of microstructural integrity associated with long-term environmental exposure and aging. Therefore, hardness measurements can serve as a meaningful complementary parameter for evaluating the relative aging condition of Bakelite-based aerospace electrical insulation components.

3.4. Differential scanning calorimetry (DSC) results

The DSC thermograms presented in Figure 4 (a) reveal a highly systematic evolution of the thermal response of the Bakelite samples with aging, particularly within the β-transition region (80–91 °C) and the principal degradation region (189–200 °C). These two thermal domains provide complementary information regarding molecular mobility, cross-link integrity, oxidative degradation, and residual structural stability of the phenol–formaldehyde network. The observed thermal behavior is fully consistent with degradation mechanisms reported for phenolic thermosets used in high-temperature engineering and aerospace environments, where long-term exposure to oxygen, humidity, and thermal cycling progressively alters the polymeric network structure (Tsiamis et al., 2019).

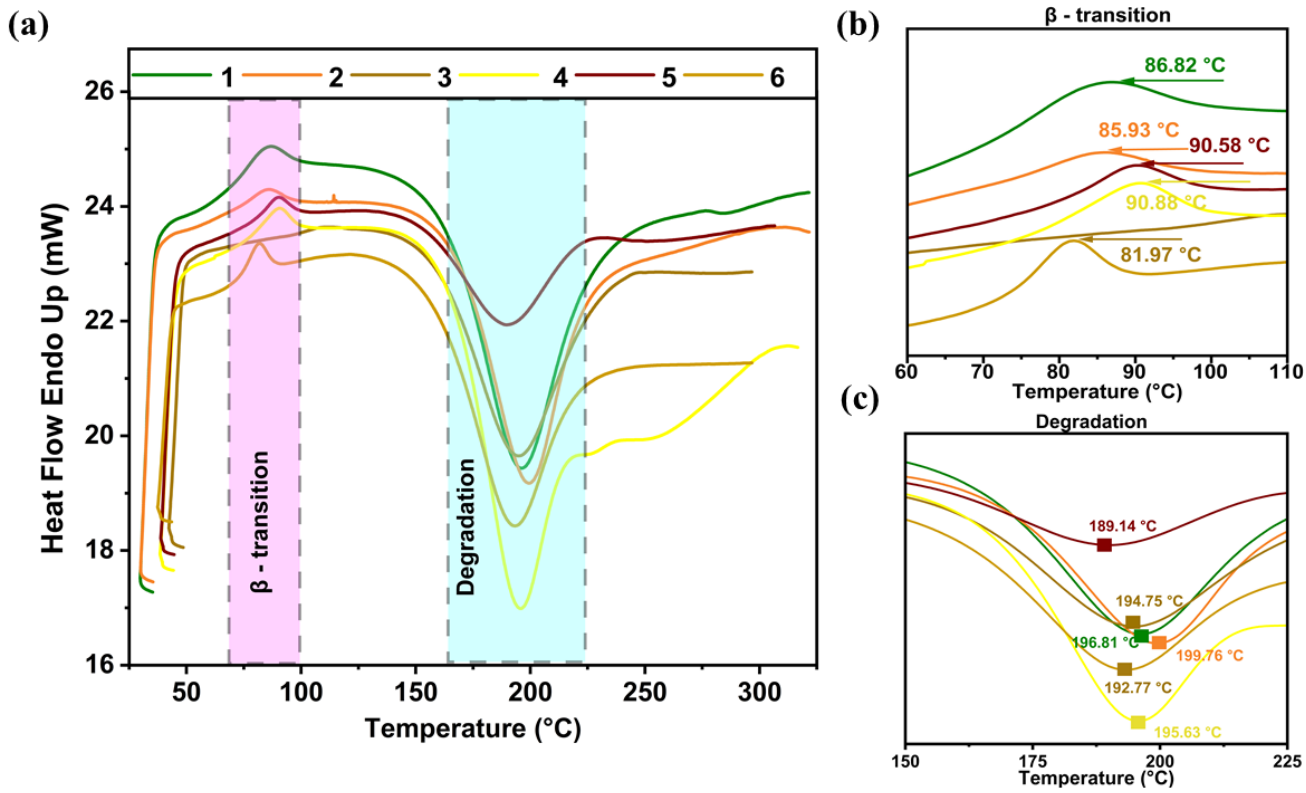


Figure 4. (a) DSC thermograms of Bakelite samples, (b) enlarged view of the β-transition behavior, and (c) degradation peak characteristics associated with thermo-oxidative aging.

In the β-transition region, as seen in Figure 4 (b), all samples exhibit a relatively broad endothermic feature between approximately 80 and 95 °C. This thermal event may be associated with a combination of moisture desorption, release of residual volatile species, and localized molecular relaxation phenomena within the cross-linked phenolic structure. However, significant differences in transition temperature and peak shape are evident among the samples. Sample 1 exhibits a β-transition temperature of approximately 86.82 °C, while Samples 2 and 3 display slightly lower transition temperatures of 85.93 °C and 81.97 °C, respectively. In contrast, Samples 4 and 6 show higher transition temperatures, approximately 90.88 °C and 90.58 °C, respectively. The β-transition value of Sample 5 could not be clearly resolved from the enlarged thermogram. The shift toward higher transition temperatures in Samples 4 and 6 may indicate reduced molecular mobility associated with aging-induced structural rearrangements and increased network rigidity within the phenolic matrix. The upward shift of the β-transition temperature in the latter samples indicates increased structural rigidity and reduced molecular mobility, which are commonly associated with oxidative aging and secondary cross-linking reactions in thermoset polymers. Similar behavior has been reported for aged phenolic systems, where prolonged environmental exposure reduces free volume and increases chain stiffness (Yu et al., 2022).

Equally important is the evolution of peak morphology within this transition region. Samples 1 and 2 exhibit broader, smoother transitions, suggesting a relatively heterogeneous yet still mobile polymer network. Conversely, Samples 4 and 5 exhibit narrower, more constrained β-transition features, implying reduced relaxation capability and advanced structural embrittlement. In thermosetting phenolic materials, narrowing of relaxation transitions is generally interpreted as evidence of reduced configurational freedom and progressive aging-induced stiffening (Bellinetto et al., 2024). Therefore, the β-transition results strongly suggest that Samples 4 and 5 have undergone more extensive physicochemical aging than Samples 1 and 2.

The most critical information for lifetime assessment, however, emerges from the principal degradation region between approximately 170 and 210 °C (Figure 4 (c)). All samples exhibit a pronounced endothermic degradation minimum associated with scission of methylene bridges, cleavage of phenolic cross-links, and oxidative decomposition of the polymeric network. The degradation peak temperature varies systematically among the samples, indicating differences in residual thermal stability. Sample 5 shows the lowest degradation minimum at approximately 189.14 °C, whereas Samples 1–4 exhibit minima between 194 and 200 °C. Sample 4 demonstrates the deepest degradation peak, centered near 195.63 °C, accompanied by the largest decrease in heat flow intensity.

The shift of degradation minima toward lower temperatures is a well-established indicator of advanced aging because oxidized and partially degraded polymer networks require less thermal energy for bond rupture. Veedu et al. have demonstrated that thermal aging reduces activation energy and accelerates decomposition kinetics due to progressive weakening of methylene bridges and oxidation-sensitive sites (Veedu et al., 2013). Consequently, the lower degradation onset observed for Sample 5 strongly indicates a more advanced degradation state and reduced remaining service life.

The degradation peak depth and width provide additional quantitative insight into aging severity. Sample 4 exhibits the deepest and broadest degradation event, reaching nearly 17 mW, whereas Samples 1 and 2 remain comparatively shallower (19–20 mW). A deeper endothermic minimum reflects greater enthalpic demand associated with large-scale bond cleavage and decomposition, while peak broadening indicates increasing heterogeneity of degradation pathways. In aged thermosetting polymers, broad degradation peaks are generally attributed to nonuniform oxidation and spatially heterogeneous chain scission caused by long-term environmental exposure (Varshney et al., 2013). Therefore, the pronounced broadening observed in Sample 4 suggests severe oxidative aging and highly heterogeneous structural deterioration.

Another important feature is the post-degradation recovery behavior above 220 °C. Samples 1 and 5 recover to relatively high heat-flow levels after the degradation minimum, whereas Samples 4 and 6 exhibit incomplete recovery and remain at lower heat-flow baselines. This behavior reflects differences in residual char-forming capability and structural integrity. Phenolic materials are known for their carbonization tendency and thermal resilience at elevated temperatures, particularly in aerospace applications (Tsiamis et al., 2019). However, prolonged aging progressively diminishes the ability of the network to reorganize into thermally stable aromatic structures, resulting in incomplete thermal recovery. The suppressed recovery observed in Sample 4, therefore, supports the conclusion of extensive network degradation.

When the β-transition behavior and degradation characteristics are considered together, a coherent aging sequence emerges. Samples 1 and 2 retain relatively high molecular mobility, higher degradation temperatures, and shallower degradation minima, indicating comparatively preserved network structures. Samples 4 and 5 exhibit increased rigidity, lower degradation stability, and more pronounced enthalpic degradation events, characteristic of advanced oxidative aging. Sample 6 deviates partially from the general trend, suggesting that it may have been subjected to different aging conditions, such as prolonged thermo-oxidative exposure, increased moisture interaction, or extended exposure to sunlight and ultraviolet radiation. These factors are known to influence degradation kinetics and thermal response in phenolic resin systems, potentially leading to aging pathways that differ from those observed in the remaining samples (Koizumi et al., 2010).

The DSC results demonstrate that the thermal event observed in the 80–95 °C region, together with degradation peak temperature, peak depth, and peak broadening, collectively constitute sensitive indicators of aging in aerospace-grade Bakelite materials. The combination of reduced degradation temperature, increased peak broadening, and suppressed post-degradation recovery provides strong evidence of progressive oxidative and thermo-mechanical aging. These findings confirm that DSC-derived thermodynamic parameters can serve as a robust framework for lifetime prediction and residual life assessment of phenolic thermoset systems employed in aerospace environments.

3.5. SEM-EDS results

Figure 5, SEM micrographs of Sample 1 and Sample 2, reveal relatively preserved and continuous phenolic network morphologies, supporting the conclusion derived from DSC and VOC analyses that these samples represent earlier aging stages. The Sample 1 micrograph exhibits a more compact and interconnected phase distribution with fewer discontinuities and void-like defects, whereas Sample 2 shows slightly increased heterogeneity and darker dispersed regions, indicating the onset of localized structural degradation. In phenolic thermosets, progressive aging is known to induce microcrack formation, phase separation, and morphological heterogeneity due to oxidative chain scission and cross-link deterioration. Therefore, the comparatively homogeneous morphology of Sample 1 suggests a less degraded microstructure relative to Sample 2.

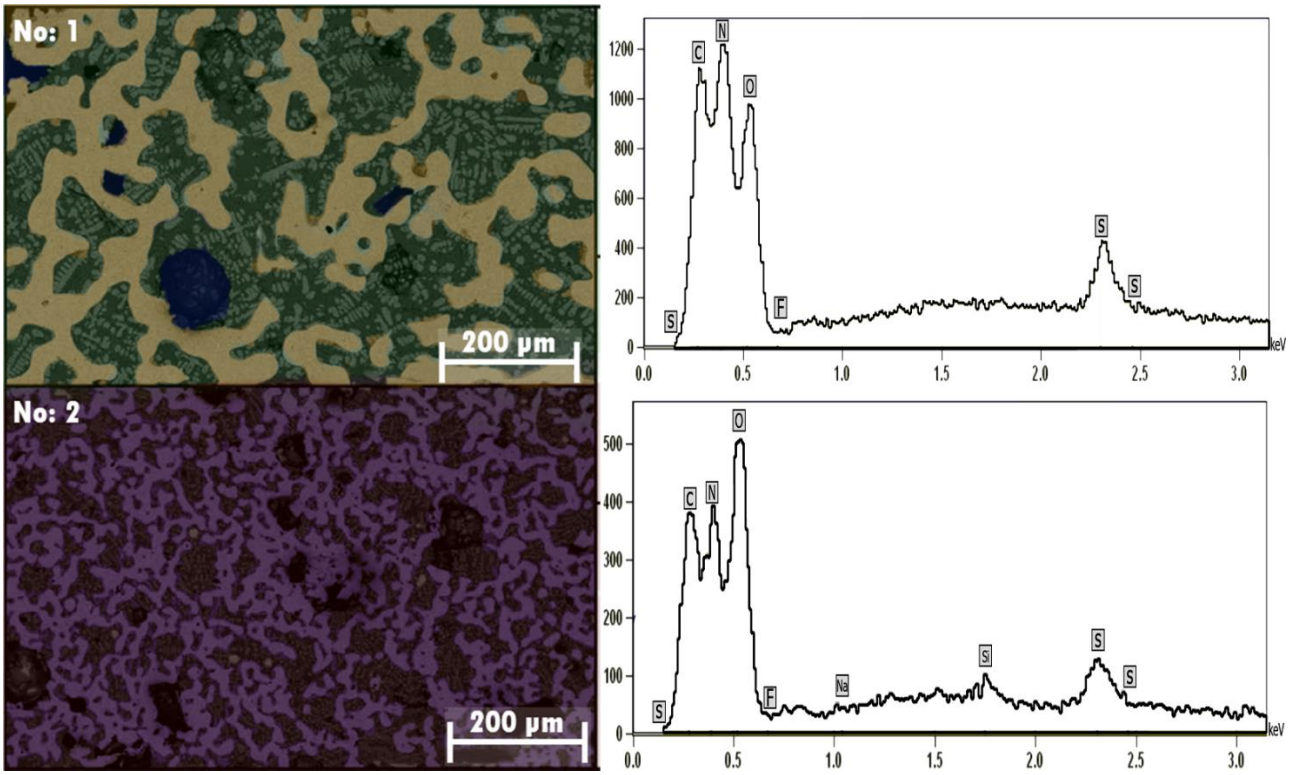


Figure 5. SEM micrographs and corresponding EDS spectra of Bakelite Samples 1 and 2, showing relatively preserved phenolic network morphology and early-stage oxidative degradation features

EDS spectra further support this interpretation. Both samples are dominated by carbon (C), nitrogen (N), and oxygen (O), consistent with the chemical structure of phenol–formaldehyde-based materials. However, Sample 2 exhibits relatively higher oxygen intensity and detectable inorganic contributions (Na and Si), suggesting increased oxidative exposure and possible environmental contamination or filler exposure associated with aging. Elevated oxygen content in aged phenolic systems is commonly linked to oxidation-induced formation of oxygen-containing functional groups and surface degradation. Additionally, sulfur-related peaks observed in both spectra may indicate residual additives or flame-retardant constituents frequently encountered in aerospace-grade phenolic composites.

SEM micrographs of Sample 5 and Sample 6, as shown in Figure 6, reveal substantially more advanced morphological deterioration than in other Samples, consistent with the FT-IR, DSC, VOC, and Shore D results, which indicate a more severe aging state. Sample 5 exhibits pronounced phase segregation, surface coarsening, and the formation of large particulate agglomerates distributed across the matrix. Such heterogeneous morphology is characteristic of oxidative aging and cross-link degradation in phenolic thermosets, where long-term environmental exposure progressively disrupts the continuity of the polymer network. The corresponding EDS spectrum is dominated by O, Na, S, and Cl, while the relative carbon signal is comparatively reduced. Increased oxygen intensity is particularly significant, as oxygen enrichment is widely recognized as a direct indicator of oxidative degradation and formation of oxygen-containing functional groups in aged phenolic systems.

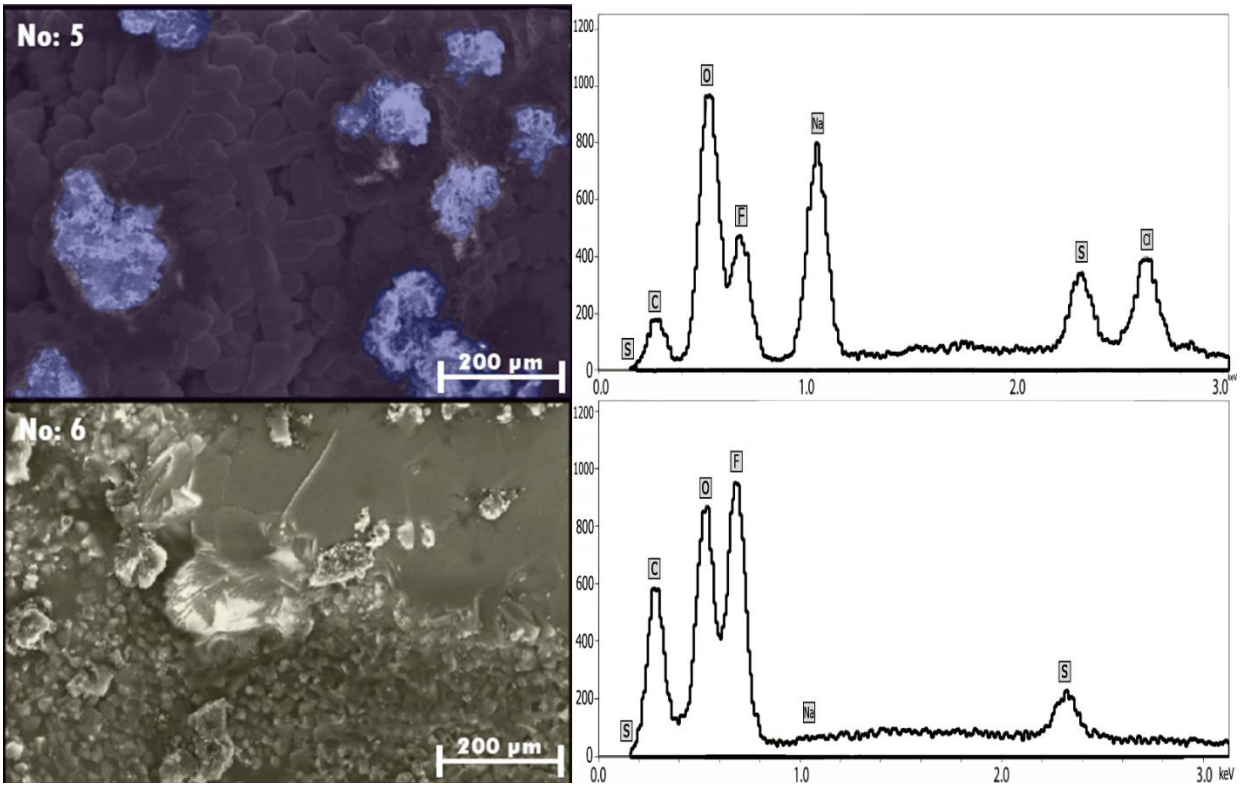


Figure 6. SEM micrographs and corresponding EDS spectra of Bakelite Samples 5 and 6, showing pronounced surface heterogeneity, fragmentation, elemental redistribution, and advanced oxidative degradation features.

Sample 6 demonstrates even more severe surface disruption, with extensive fragmentation, brittle particulate structures, and highly irregular topography. Unlike the relatively continuous morphology observed in Samples 1 and 2, the matrix integrity in Sample 6 appears significantly compromised, suggesting advanced chain scission and loss of cohesive cross-linked structure. The EDS spectrum of Sample 6 shows strong oxygen and fluorine signals together with sulfur contributions, while sodium intensity decreases substantially relative to Sample 5. The elevated fluorine-related signal may indicate exposure-related additive migration or degradation of fluorinated constituents associated with aerospace service environments. Similar elemental redistribution phenomena have been reported in aged high-performance thermosetting composites subjected to prolonged thermo-oxidative exposure.

The elevated O, F, Na, and Cl signals observed in Samples 5 and 6 are believed to be associated with long-term environmental exposure, oxidation-induced surface modification, and the progressive exposure of inorganic constituents previously embedded within the phenolic matrix. As thermo-oxidative aging proceeds, degradation of the polymer network may increase the relative contribution of inorganic phases and environmentally accumulated species in the EDS spectra. Therefore, the observed elemental enrichment is interpreted as an aging-related surface phenomenon rather than direct evidence of external chemical contamination.

The SEM–EDS findings strongly corroborate the previously obtained FT-IR, DSC, VOC, and Shore D results. Samples 1 and 2 retained comparatively homogeneous morphologies, lower oxygen enrichment, and more intact phenolic network structures, indicating earlier aging stages. In contrast, Samples 5 and 6 exhibited substantial morphological heterogeneity, particle agglomeration, brittle fracture features, and elevated oxygen-containing species, all of which are consistent with advanced thermo-oxidative degradation. The progressive transition from structurally continuous morphologies (Samples 1–2) to fragmented and oxidized surfaces (Samples 5–6) provides direct microstructural evidence for aging progression in the Bakelite materials. Collectively, the combined thermal, chemical, mechanical, and microstructural analyses demonstrate a coherent degradation pathway governed primarily by oxidation-induced cross-link deterioration and environmental aging (Yu et al., 2018, 2022).

3.6. Age calculation using Bayesian probability models

This model aims to determine the most likely age range by evaluating the available FT-IR, DSC, Shore D, VOC/GC-MS, and SEM-EDS findings together. This approach is consistent with the literature showing that aging in phenol-formaldehyde/Bakelite-type materials is monitored using FT-IR, VOC, thermal analysis, and morphology; however, because there is no universal age equation in the literature that directly maps years to spectra, the model is range-based and probabilistic (Pintar et al., 2020).

As defined in Equation (1), three age ranges were considered with equal prior probabilities. H1: Materials 0-20 years, H2: Materials 20-40 years, H3: Materials 40-60 years. Here, the term "materials" refers to the overall age range of the entire sample set. Initially, equal priority was given to the three hypotheses.

$$P(H1) = P(H2) = P(H3) = \frac{1}{3} \quad (1)$$

Initially, no age group was considered superior to another. Equal prior probabilities were assigned because the manufacturing dates and pre-installation storage histories of the investigated components were unavailable. The conditional probabilities assigned to the six experimental observations are given in Equations (2)–(7). Although the aircraft has remained in service for approximately 30 years, the actual age of an individual Bakelite component may differ substantially from the aircraft service age due to unknown storage durations before installation. To avoid introducing preferential bias toward any specific age interval, all three age hypotheses were therefore assigned equal prior probabilities at the beginning of the Bayesian analysis.

Experimental Findings Reduced to Six Primary Evidence Categories. E1: Significant oxidation in FT-IR, but graded across samples; E2: Volatile reduction and oxidative product dominance in advanced samples in VOC/GC findings; E3: Moderate-to-advanced irregularity in DSC, but not complete collapse; E4: Increased cracking/deterioration in SEM, but not uniform across all samples; E5: Limited decrease in hardness in Shore D, meaning the material is aged but does not appear to be completely severely weathered; E6: Distribution Structure of the Sample Set.

The conditional probabilities assigned to each evidence category were established using a semi-quantitative expert-based evaluation of the experimental findings. FT-IR, VOC/GC-MS, DSC, SEM-EDS, hardness, and sample-distribution characteristics were collectively interpreted according to their consistency with degradation patterns expected for each age interval. Higher conditional probabilities were assigned when the observed degradation indicators showed stronger agreement with the expected characteristics of a given age hypothesis, whereas lower values reflected weaker agreement. Therefore, the assigned probabilities should be interpreted as relative confidence levels derived from experimental observations rather than directly measured statistical frequencies.

Evidence 1: FT-IR oxidation pattern
The results show oxidation, but it does not exhibit very advanced terminal degradation; furthermore, there is diffusion between samples.

$$P(E1|H1) = 0.55,\ P(E1|H2) = 0.70,\ P(E1|H3) = 0.85 \quad (2)$$

Evidence 2: VOC/GC pattern
Since volatiles decreased and oxidative products became dominant in the more advanced samples, and less aging was observed in the lighter samples, this is again most consistent with H2.

$$P(E2|H1) = 0.50,\ P(E2|H2) = 0.68,\ P(E2|H3) = 0.82 \quad (3)$$

Evidence 3: DSC behavior
There is significant aging in the DSC, but not all samples show excessive thermal degradation. This supports H2.

$$P(E3|H1) = 0.58,\ P(E3|H2) = 0.72,\ P(E3|H3) = 0.84 \quad (4)$$

Evidence 4: SEM EDS morphology
In SEM EDS, cracking and heterogeneous deformation are increased, but not all samples are "severely fragmented". Therefore, H2 is still optimum.

$$P(E4|H1) = 0.52,\ P(E4|H2) = 0.70,\ P(E4|H3) = 0.80 \quad (5)$$

Evidence 5: Hardness - Shore D
Hardness has decreased, but phenolic thermoset rigidity is still maintained. This does not completely rule out H1, but it is better compatible with H2 and moderately compatible with H3.

$$P(E5|H1) = 0.65,\ P(E5|H2) = 0.60,\ P(E5|H3) = 0.78 \quad (6)$$

Evidence 6: Distribution structure of the sample set.

$$P(E6|H1) = 0.40,\ P(E6|H2) = 0.85,\ P(E6|H3) = 0.55 \quad (7)$$

The combined likelihood for each hypothesis was calculated using Equation (8). The resulting likelihoods for the three hypotheses are presented in Equations (9)–(11).

$$P(E|H_i) = \prod_{k=1}^{6} P(E_k \mid H_i) \quad (8)$$

$$P(E|H1) = 0.55\times0.50\times0.58\times0.52\times0.65\times0.40 = 0.0216 \quad (9)$$

$$P(E|H2) = 0.70\times0.68\times0.72\times0.70\times0.60\times0.85 = 0.1224 \quad (10)$$

$$P(E|H3) = 0.85\times0.82\times0.84\times0.80\times0.78\times0.55 = 0.2009 \quad (11)$$

The unnormalized posterior probabilities were then calculated using Equations (12)–(15).

$$P(H1)P(E|H1) = \frac{1}{3}\times0.0216 = 0.0072 \quad (12)$$

$$P(H2)P(E|H2) = \frac{1}{3}\times0.1224 = 0.0408 \quad (13)$$

$$P(H3)P(E|H3) = \frac{1}{3}\times0.2009 = 0.0670 \quad (14)$$

$$= 0.0072+0.0408+0.0670= 0.1150 \quad (15)$$

The final Bayesian results, obtained after normalization, are presented in Equations (16)–(18).

$$P(H1|E) = 0.062 = 6.2\% \quad (16)$$

$$P(H2|E) = 0.355 = 35.5\% \quad (17)$$

$$P(H3|E) = 0.582 = 58.3\% \quad (18)$$

4. Discussion

The combined characterization results indicate that the aging behavior of the investigated aerospace Bakelite materials cannot be attributed to a single degradation mechanism but rather to the cumulative effects of long-term thermo-oxidative aging. The consistency observed among FT-IR, DSC, GC-MS, Shore D, and SEM-EDS findings suggests that chemical oxidation, progressive modification of the phenolic network structure, volatile depletion, and microstructural deterioration occur simultaneously and reinforce one another throughout the aging process. Similar multi-stage degradation pathways have been reported for phenolic thermosets exposed to prolonged environmental and thermal stress, where oxidation-induced changes gradually reduce thermal stability, alter mechanical behavior, and promote structural heterogeneity. Therefore, agreement among the different characterization techniques provides a coherent interpretation of the degradation state of the investigated materials and supports an integrated multi-parameter assessment strategy for aging evaluation.

One of the most significant contributions of this study is implementing a Bayesian probabilistic framework for age estimation using multidimensional characterization data. Unlike deterministic approaches relying on a single analytical parameter, the present methodology integrates multiple degradation indicators within a probabilistic decision structure, enabling a more realistic interpretation of aging uncertainty. The Bayesian model showed that the hypothesis corresponding to the 40–60 year age interval achieved the highest posterior probability (58.3%), while the 0–20 and 20–40 year hypotheses remained substantially less probable. This result is highly consistent with the experimental findings, particularly the advanced oxidation patterns observed in FT-IR, the severe thermal degradation behavior identified by DSC, and the pronounced morphological deterioration detected in SEM-EDS analyses for Samples 5 and 6. Nevertheless, the study also demonstrates that aging behavior is not fully homogeneous among the samples, indicating that environmental history, operational exposure, and possible formulation differences may influence degradation progression. Therefore, the proposed Bayesian approach should not be interpreted as an exact chronological dating method, but rather as a scientifically grounded probabilistic aging assessment framework. From an aerospace maintenance perspective, this approach provides a practical and highly valuable tool for evaluating residual serviceability, maintenance prioritization, and failure risk assessment of aging phenolic insulation materials used in aircraft electrical systems. It should also be emphasized that the Bayesian result is dependent on the predefined age hypotheses and the semi-quantitative conditional probabilities assigned to the experimental evidence. Therefore, the posterior probability of 58.3% for the 40–60 year interval should not be considered an independent validation of exact chronological age. Instead, it represents the most probable degradation-based age category under the assumptions and evidence structure defined in this study. In addition, Sample 6 did not fully follow the general degradation trend observed in the other samples. Its GC-MS profile showed the absence of detectable phenol/cresol derivatives and light aromatic compounds, while furfural derivatives and aliphatic hydrocarbons remained present. Similarly, its DSC response indicated incomplete post-degradation recovery. These deviations suggest that Sample 6 may have experienced a different storage, formulation, or environmental exposure history compared with the other samples.

5. Conclusions and Design Lessons

This study demonstrates that aerospace Bakelite components can be evaluated using a multi-parameter aging assessment framework combining FT-IR, DSC, Shore D hardness, GC-MS/VOC analysis, and SEM-EDS. The most relevant experimental indicators were the progressive loss of hydroxyl and methylene bridge-related FT-IR bands, increased carbonyl formation, reduction of VOC content,

changes in DSC degradation behavior, Shore D hardness variation, and oxygen-enriched microstructural deterioration. The GC-MS results showed a marked decrease in total VOC content from approximately 150 µg/g in Sample 1 to 40 µg/g in Sample 5, corresponding to an approximately 73% reduction. Furfural derivatives decreased from approximately 80 µg/g to 25 µg/g, corresponding to an approximately 69% reduction. DSC analysis showed degradation minima within approximately 189–200 °C, with Sample 5 showing the lowest degradation temperature. Shore D hardness values remained within the 81.4–88.4 Shore D range, indicating that the thermoset rigidity was partially preserved despite chemical and microstructural degradation.

The Bayesian probability model provided a quantitative framework for interpreting these multidimensional findings. Among the three proposed age hypotheses, the 40–60 year interval showed the highest posterior probability, with a calculated likelihood of 58.3%, whereas the 0–20 year and 20–40 year intervals remained considerably lower at 6.2% and 35.5%, respectively. Therefore, under the assumptions and evidence-weighting structure adopted in this study, the investigated Bakelite materials are most consistently associated with the 40–60-year degradation-based age category. However, this result should be interpreted as a probabilistic age-range assessment rather than an exact chronological dating method, since formulation differences, service environment, thermal history, humidity exposure, and filler content may influence degradation behavior.
From a practical design and maintenance perspective, the main lesson is that aged Bakelite components should not be assessed only by visual inspection or hardness measurement. Although the samples preserved their general thermoset rigidity, chemical and microstructural degradation indicators revealed substantial internal and surface aging. This means that aerospace Bakelite components may appear mechanically intact while already showing chemical oxidation, reduced thermal stability, and microcrack formation. Therefore, maintenance decisions for older phenolic insulation components should be based on combined chemical, thermal, mechanical, and microstructural evidence.

The study shows that a Bayesian, evidence-integrated approach can provide a more realistic and defensible aging assessment than a single-method interpretation. For aerospace electrical insulation systems, this approach can support maintenance prioritization, replacement decisions, and residual serviceability evaluation of aged Bakelite components. Future work should include reference Bakelite samples with known service histories, larger sample populations, TGA/DMA validation, and quantitative FT-IR/GC-MS indices to further improve the reliability of probabilistic age estimation.

Author Contributions

Conceptualization, methodology, modeling, controller design, simulation framework, analysis, and manuscript preparation were carried out by C. Bilgi.

Compliance with ethical standards

The author declares no conflict of interest and confirms that no human or animal subjects were involved in this study.

Data Availability Statement

All relevant experimental data, characterization results, and probabilistic modeling outputs supporting the conclusions of this study are available from the corresponding author upon reasonable request.

Conflict of Interest

The author declares that they have no known competing financial interests or personal relationships that could have appeared to influence the work reported in this paper.

Ethical approval

This study did not involve human participants, human data, or animal experiments. Therefore, formal ethical committee approval was not required.

References

An, Z., Xu, Z., Ye, Y., & Yang, R. (2021). A rapid and highly sensitive evaluation of polymer composite aging with linear correlation to real-time aging. Analytica Chimica Acta, 1169, 338632. https://doi.org/10.1016/j.aca.2021.338632

Aronovich, D. A., & Petrova, A. P. (2023). Modern phenolic adhesives for aviation and engineering. Part 1. The effect of modifying additives. Polymer Science, Series D, 16(3), 777–792. https://doi.org/10.1134/s1995421223030024

Asim, M., Saba, N., Jawaid, M., Nasir, M., Pervaiz, M., & Alothman, O. Y. (2018). A review on phenolic resin and its composites. Current Analytical Chemistry, 14(3), 185–197. https://doi.org/10.2174/1573411013666171003154410

Bellinetto, E., Fumagalli, N., Astorri, M., Turri, S., & Griffini, G. (2024). Elucidating the role of lignin type and functionality in the development of high-performance biobased phenolic thermoset resins. ACS Applied Polymer Materials, 6(2), 1191–1203. https://doi.org/10.1021/acsapm.3c02136

Bilgi, C., Demir, B., Ahlatci, H., Akin, B., Özdemir, Y., Keskin, E., & Unver, R. T. (2025). Wear behavior of aviation-grade epoxy nanocomposites reinforced with functionalized graphene nanoplatelets. Polymer Composites, 46(17), 16260–16277. https://doi.org/10.1002/pc.70043

Bilgi, C., Pektürk, H. Y., & Demir, B. (2025). Improvement of mechanical performance via interfacial strengthening of carbon fiber-epoxy reinforced hybrid laminate by incorporation of functionalized graphene nanoplatelet interphase. Polymer Composites, 46(5), 4614–4629. https://doi.org/10.1002/pc.29264

Breuer, U. P. (2016). Commercial aircraft composite technology. Springer International Publishing. https://doi.org/10.1007/978-3-319-31918-6

Campanale, C., Savino, I., Massarelli, C., & Uricchio, V. F. (2023). Fourier transform infrared spectroscopy to assess the degree of alteration of artificially aged and environmentally weathered microplastics. Polymers, 15(4), 911. https://doi.org/10.3390/polym15040911

Curran, K., Underhill, M., Gibson, L. T., & Strlic, M. (2016). The development of a SPME-GC/MS method for the analysis of VOC emissions from historic plastic and rubber materials. Microchemical Journal, 124, 909–918. https://doi.org/10.1016/j.microc.2015.08.027

De Florio, F. (2011). Airworthiness: An introduction to aircraft certification. Butterworth-Heinemann. https://doi.org/10.1016/c2010-0-65567-2

Demleitner, M., Albuquerque, R. Q., Sarhadi, A., Ruckdäschel, H., & Eder, M. A. (2024). Bayesian optimization-based prediction of the thermal properties from fatigue test IR imaging of composite coupons. Composites Science and Technology, 248, 110439. https://doi.org/10.1016/j.compscitech.2024.110439

Dogru, A., Bilgi, C., Sözen, A., & Mavi, F. (2026). Assessing the performance characteristics of aluminum-doped PLA composites after exposure to environmental conditions. Journal of Thermoplastic Composite Materials, 39(7), 3837–3865. https://doi.org/10.1177/08927057251408696

Ece, A., Yılmaz, A., & Civalek, Ö. (2025). A brief introduction to the properties of aerospace materials. International Journal of Engineering and Applied Sciences, 17(1), 44–60. https://doi.org/10.24107/ijeas.1640337

Erzen, B., Karataş, M., Deniz, Ş., & Aydoğmuş, E. (2024). Advances in synthesis, characterization, and industrial applications of phenol formaldehyde resins. International Journal of Advanced Natural Sciences and Engineering Researches, 8(4), 26–34. https://www.as-proceeding.com/index.php/ijanser/article/view/1817

Guseva, O., Brunner, S., & Richner, P. (2003). Service life prediction for aircraft coatings. Polymer Degradation and Stability, 82(1), 1–13. https://doi.org/10.1016/s0141-3910(03)00124-1

Haka, A. T. (2023). Composites in 20th-century polymer chemistry. In Engineered stability: The history of composite materials in the 19th and 20th centuries (pp. 113–255). Springer. https://doi.org/10.1007/978-3-658-41408-5_4

Jewell, B., Abadi, P. P., & Sain, T. (2025). Experimental characterization and constitutive modeling of bulk epoxy under thermo-oxidative aging. Polymer Degradation and Stability, 234, 1–19. https://doi.org/10.1016/j.polymdegradstab.2025.111215

Koizumi, K., Charles, T., & De Keyser, H. (2010). Phenolic molding compounds. In L. Pilato (Ed.), Phenolic resins: A century of progress (pp. 383–437). Springer Berlin Heidelberg. https://doi.org/10.1007/978-3-642-04714-5_16

Koley, R., Kasilingam, R., Sahoo, S., Chattopadhyay, S., & Bhowmick, A. K. (2019). Synthesis and characterization of phenol furfural resin from moringa oleifera gum and biophenol and its application in styrene butadiene rubber. Industrial & Engineering Chemistry Research, 58(40), 18519–18532. https://doi.org/10.1021/acs.iecr.9b03684

Lizcano, M., Williams, T. S., Shin, E. S. E., Santiago, D., & Nguyen, B. (2022). Aerospace environmental challenges for electrical insulation and recent developments for electrified aircraft. Materials, 15(22), 8121. https://doi.org/10.3390/ma15228121

Lobanova, M., Aleshkevich, V., Babkin, A., Kepman, A., Avdeev, V., Morozov, O., & Bulgakov, B. (2023). Effect of post-curing temperature on the retention of mechanical strength of phthalonitrile thermosets and composites after a long-term thermal oxidative aging. Polymer Composites, 44(12), 8330–8343. https://doi.org/10.1002/pc.27699

Ma, J., Wu, W., Ke, Z., Li, H., Luo, J., Yang, J., & Liu, G. X. (2022). Viscosity master curves and predictions of phenolic resin solutions through early aging. Polymer, 261, 125405. https://doi.org/10.1016/j.polymer.2022.125405

Mitu, B., Trojan, V., Hrib, R., & Halámková, L. (2025). Attenuated total reflection Fourier transform infrared spectroscopy (ATR-FTIR) analysis of human nails: Implications for age determination in forensics. Journal of Forensic Sciences, 70(1), 150–160. https://doi.org/10.1111/1556-4029.15641

Özsin, G. (2025). Exploring the thermal degradation of Bakelite: Non-isothermal kinetic modeling, thermodynamic insights, and evolved gas analysis via integrated in situ TGA/MS and TGA/FT-IR techniques. Polymers, 17(16), 2197. https://doi.org/10.3390/polym17162197

Pintar, A. L., White, C. C., & Sung, L. P. (2020). Bayesian hierarchical models for service-life prediction of polymers. In S. Ebnesajjad (Ed.), Service life prediction of polymers and coatings (209–231). William Andrew Publishing. https://doi.org/10.1016/b978-0-12-818367-0.00011-4

Popa, G. N., Nikolov, D. A., & Diniș, C. M. (2024). About the aged degradation of the materials used for medium-voltage distributors. Energies, 17(14), 3418. https://doi.org/10.3390/en17143418

Qi, H. J., Joyce, K., & Boyce, M. C. (2003). Durometer hardness and the stress-strain behavior of elastomeric materials. Rubber Chemistry and Technology, 76(2), 419–435. https://doi.org/10.5254/1.3547752

Ravindran, L., Sreekala, M. S., Kumar, A. S., & Thomas, S. (2022). A comprehensive review on phenol-formaldehyde resin-based composites and foams. Polymer Composites, 43(12), 8602–8621. https://doi.org/10.1002/pc.27059

Strzemiecka, B., Voelkel, A., Zieba-Palus, J., & Lachowicz, T. (2014). Assessment of the chemical changes during storage of phenol-formaldehyde resins pyrolysis gas chromatography mass spectrometry, inverse gas chromatography and Fourier transform infrared methods. Journal of Chromatography A, 1359, 255–261. https://doi.org/10.1016/j.chroma.2014.07.045

Tian, R., Li, K., Lin, Y., Lu, C., & Duan, X. (2023). Characterization techniques of polymer aging: from beginning to end. Chemical Reviews, 123(6), 3007–3088. https://doi.org/10.1021/acs.chemrev.2c00750

Tsiamis, A., Iredale, R. J., Backhouse, R., Hallett, S. R., & Hamerton, I. (2019). Liquid processable, thermally stable, hydrophobic phenolic triazine resins for advanced composite applications. ACS Applied Polymer Materials, 1(6), 1458–1465. https://doi.org/10.1021/acsapm.9b00212

Uddin, F. (2016). Flame-retardant fibrous materials in an aircraft. Journal of Industrial Textiles, 45(5), 1128–1169. https://doi.org/10.1177/1528083714540700

van de Schoot, R., Depaoli, S., King, R., Kramer, B., Märtens, K., Tadesse, M. G., Vannucci, M., Gelman, A., Veen, D., Willemsen, J., & Yau, C. (2021). Bayesian statistics and modelling. Nature Reviews Methods Primers, 1, Article 1. https://doi.org/10.1038/s43586-020-00001-2

Varshney, P., Gururani, S. K., Singh, R., & Zaidi, M. G. H. (2013). Recent advances in thermal analysis of polymers, copolymers and related polymer composites (A review). Materials Science Research India, 4(2), 353–372. https://doi.org/10.13005/msri/040217

Veedu, A. K. K., Basavaraju, R. H., & Chikkakuntappa, R. (2013). Thermally induced microstructural changes and its influence on electrical conductivity of a polymer-based bakelite RPC detector material: A positron lifetime study. Journal of Applied Polymer Science, 130(2), 793–800. https://doi.org/10.1002/app.39234

Wilson, D., & Allen, C. (2017). A Bayesian estimation model for transient engine exhaust characterization using Fourier transform infrared spectroscopy. Energy and Fuels, 31(10), 11156–11168. https://doi.org/10.1021/acs.energyfuels.7b02224

Yang, X., Zhi, M., Li, Y., Xin, H., Fan, R., Chen, X., Liu, Q., & He, Y. (2023). Improved flame retardancy and smoke suppression properties of phenolic resin by incorporating MoO3 particles. High Performance Polymers, 35(6), 559–570. https://doi.org/10.1177/09540083231153336

Yu, Y., Li, C., Jiang, C., Chang, J., & Shen, D. (2022). Aging behaviors of phenol-formaldehyde resin modified by bio-oil under five aging conditions. Polymers, 14(7), 1352. https://doi.org/10.3390/polym14071352

Yu, Y., Xu, P., Chang, M., & Chang, J. (2018). Aging properties of phenol-formaldehyde resin modified by bio-oil using UV weathering. Polymers, 10(11), 1183. https://doi.org/10.3390/polym10111183

Zhang, K., Wang, Z., Nie, J., & Wen, F. (2024). Study on combustion characteristics of glass fiber/phenolic resin composites. Heliyon, 10(13), e32939. https://doi.org/10.1016/j.heliyon.2024.e32939

Zhao, W., Hsu, S. L., Ravichandran, S., & Bonner, A. M. (2019). Moisture effects on the physical properties of cross-linked phenolic resins. Macromolecules, 52(9), 3367–3375. https://doi.org/10.1021/acs.macromol.9b00385

Zheng, F., Ren, Z., Xu, B., Wan, K., Cai, J., Yang, J., Zhang, T., Wang, P., Niu, B., Zhang, Y., & Long, D. (2021). Elucidating multiple-scale reaction behaviors of phenolic resin pyrolysis via TG-FTIR and ReaxFF molecular dynamics simulations. Journal of Analytical and Applied Pyrolysis, 157, 105222. https://doi.org/10.1016/j.jaap.2021.105222